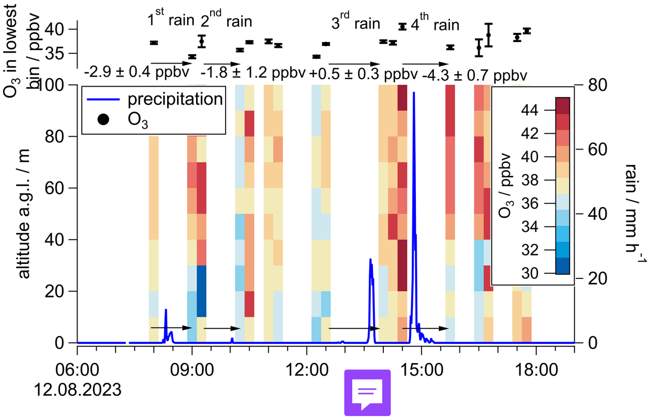

Figure 11. The vertically resolved O_3-time series (15 min-time increments with 5 m altitude TS1 resolution, color-coded, measured with FLab) shows a decrease of 3.0 ± 1.3 ppbv O_3 at the lowest bin (top panel) after rain events (blue, 60 s data) and a slow increase as O_3-rich air is injected from higher levels.

of an onset of convergence leading to more low level and convective clouds and may be enhanced by the cold pool at the ground. This downdraft results in the injection of clean, O_3-rich air with low particle load into the lowermost troposphere and represents the transition to air mass III (Figs. 8e, f and 10).

After each rain event, O_3 mixing ratios are increased at altitudes above 200 m (due to the air mass downdraft from higher altitudes, Fig. 8e), but decreased near the ground by 3.0 ± 1.3 ppbv, excluding the 10:00 rainfall, as shown in Fig. 11. As a consequence, O_3 gradients are enhanced by 7 ppbv km^{-1} for each rain event and subsequently disappear within a few hours due to convective mixing within the PBL. Reduced ground-level O_3 concentrations following rainfall may result from deposition or enhanced O_3 depletion, whereas outwash seems unlikely due to the poor solubility of O_3 in water, except for potential aqueous phase SO_2 oxidation (Hoyle et al., 2016). Depletion could be driven by the increased release of primary biogenic volatile organic compounds (BVOCs) from vegetation (Rossabi et al., 2018; Miyama et al., 2020; Machado et al., 2024a), by peroxide-scavenging after rainfall (Bela et al., 2018) or reaction with soil-emitted NO after rain (Andersen et al., 2024). BVOCs have been identified as an O_3 sink in natural and anthropogenic conditions (Fitzky et al., 2019; Machado et al., 2024a). However, this emission-driven O_3 removal mechanism cannot be verified due to the lack of BVOC and NO data.

Figure 8f highlights that for the same rain events, when O_3-rich air was injected into the lowest 500 m, the CPC PNC was consistently reduced by 25 % (except when the NBL was still present, because air mass I is already in the free troposphere). The PNC gradient remained unchanged during and after the regeneration period, and the PM_1 levels measured at ground remained constant immediately after rain (Fig. 9), indicating that washout was minimal under these conditions. This is likely due to the size of the measured aerosol particles that are in the Greenfield gap and consequentially inefficiently removed by outwash (Cherrier et al., 2017).

These observations show that rain itself does not necessarily significantly influence the distribution of pollutants such as O_3, PM_1, and PNC. However, post-rain air masses determine the composition and gradients at higher levels, while rain-induced emissions from the ground may act as a sink for reactive substances as O_3.

4.4 Influence of cold pool formation on model MLH

In Sect. 3 we showed that the determination of the MLH using 1 h forecast data from the ICON model is feasible with high accuracy under stable conditions during a weak warm front (Fig. 5). The MLH estimation criteria in the model include the Brunt–Väisälä frequency, humidity, and potential virtual temperature gradients. Until this point of the study the MLH is used as a synonym for the height of the planetary boundary layer (PBLH), which is considered the most relevant measure separating the free troposphere and the ground-influenced layer with different dynamical characteristics and compositions (Stull, 1988; Tignat-Perrier et al., 2020; Kotthaus et al., 2023). Note that other kinds of stratification occur regularly in the troposphere (even within the planetary boundary layer) and are often not predictable, due to local topography, emissions, and heat reservoirs.

For the convergence line/cold front case analyzed in this section, the modelled MLH, shown in Figs. 7a and 10, increases from 0 m at 08:30 to 200 m at 10:00 and 300 m at 11:00. This observation is consistent with the NBL identified from in-situ FLab data and demonstrates additionally to Fig. 5 that the MLH algorithm predicts the height of the NBL (in this case the PBLH) accurately. However, between 12:00 and 18:00, the modelled MLH drops below 500 m before returning to levels above 600 m at 18:00, where it continues following its diurnal cycle. The average predicted diurnal cycle of the MLH at the measurement site from Sect. 4 shows maxima of the MLH between 800 to 1000 m at 14:00 to 15:00 on clear-sky days, while being < 20 m during night (Fig. 7a). The difference between the modelled MLH in the cold front case, compared to the average diurnal cycle of the PBLH, may be explained by reduced irradiance (average of 100 W m^{-2} during this period).

The formation of a cold pool at ground leads to an increase of latent heat flux and consequentially to less turbulent mixing. Therefore, the cold pool acts as an energy sink and suppresses energy supply for further turbulent mixing. Although convection has driven the PBLH up to the free troposphere before the rain, the cold pool contributes to layering of the convective-driven RL above a shallow turbulent mixing layer. This stratification disappears as the cold pool dissolves.